

**Supporting Information**  
**Single-Molecule Analysis of Lipid-Protein Interactions In Crude Cell Lysates**  
Edwin Arauz<sup>†§</sup>, Vasudha Aggarwal<sup>‡§</sup>, Ankur Jain<sup>‡</sup>, Taekjip Ha<sup>‡||\*#</sup>, and Jie Chen<sup>†\*</sup>

<sup>†</sup>*Department of Cell and Developmental Biology*, <sup>‡</sup>*Center for Biophysics and Computational Biology*, <sup>||</sup>*Department of Physics and Center for the Physics of Living Cells, University of Illinois at Urbana-Champaign, Urbana, Illinois 61801.* <sup>#</sup>*Howard Hughes Medical Institute, Baltimore, Maryland 21205.*

<sup>§</sup>These authors contributed equally to this work

\*Corresponding authors: T.H.: [tjha@jhu.edu](mailto:tjha@jhu.edu); J.C.: [jiechen@illinois.edu](mailto:jiechen@illinois.edu)

**TABLE OF CONTENTS**

SUPPLEMENTARY METHODS.....	S-2
Figure S1. Number of DiD molecules per vesicle.....	S-4
Figure S2. Binding of tandem-repeat LBDs to their target lipids.....	S-5
Figure S3. Framework for data analysis.....	S-6
Figure S4. Binding of tandem LBDs to their target lipids.....	S-7
Figure S5. Tandem-repeat LBDs are mostly monomeric.....	S-8
Figure S6. Binding of single-copy LBDs to their target lipids.....	S-9
Figure S7. Single-copy LBDs are mostly monomeric. ....	S-10
Figure S8. Binding of Akt and Akt-PH to PIP <sub>3</sub> vesicles.....	S-11
Figure S9. Serum stimulation does not affect Akt-PIP <sub>3</sub> interaction. ....	S-12
SUPPLEMENTARY REFERENCES.....	S-13

## SUPPLEMENTARY METHODS

**Antibodies and Reagents.** Antibodies were obtained from commercial sources as follows: biotinylated rabbit anti-GFP and mouse anti-GFP for immunoblotting from Rockland Immunochemicals; biotinylated mouse anti-S473 and rabbit anti-S473 for immunoblotting from Cell Signaling Technology. 1-palmitoyl-2-oleoyl-sn-glycero-3-phosphocholine (POPC), 1-palmitoyl-2-oleoyl-sn-glycero-3-phosphate (POPA), 1-palmitoyl-2-oleoyl-sn-glycero-3-phospho-L-serine (POPS), 1,2-dioleoyl-sn-glycero-3-phospho-(1'-myo-inositol-4',5'-bisphosphate) (PIP<sub>2</sub>), 1,2-dioleoyl-sn-glycero-3-phospho-(1'-myo-inositol-3',4',5'-trisphosphate) (PIP<sub>3</sub>), and 1,2-dipalmitoyl-sn-glycero-3-phosphoethanolamine-N-(Cap Biotinyl) (biotinPE) were purchased from Avanti Lipids Inc. Phosphatidylinositol-3-phosphate (PI(3)P) was from Echelon Biosciences Inc. 1,1'-dioctadecyl-3,3',3',3'-tetramethylindodicarbocyanine perchlorate (DiD) was from Invitrogen. Purified GFP protein was from Abcam (ab84191).

**Plasmids.** The GFP-2xHrs-FYVE construct was previously reported by the Stenmark laboratory.<sup>1</sup> GFP-2xSpo20-PABD<sup>2</sup> was from the Du laboratory at The University of Texas Health Science Center at Houston. The following plasmids were obtained from Addgene: GFP-PLCd-PH (#21179),<sup>3</sup> 2xPH-PLCd-GFP (#35142),<sup>4</sup> GFP-Akt (#39531), and GFP-Akt-PH (#39533).<sup>5</sup> GFP-Akt mutants (T308D/S473D; T308A/S473A; T308A/S473D; T308D/S473A) were created using QuickChange II mutagenesis kit (Stratagene). GFP-1xSpo20-PABD and GFP-1xHrs-FYVE were created by inserting a single copy of Spo20-PABD and Hrs-FYVE, respectively, into a gateway destination plasmid pCDNA5 with AttR1/R2 recombination sites and GFP fused at the N-terminus.

**Cell Lysis.** HEK293 Cells seeded in 6-well plates were transfected at 70-80% confluence with various plasmids (3 µg each well) using PolyFect following the manufacturer's recommendation (Qiagen). After 24 hr, cells were wash twice in ice-cold PBS and re-suspended in 150 µL per well of detergent-free buffer (40 mM Hepes pH 8.0, 150 mM NaCl, 10 mM β-glycerophosphate, 10 mM sodium pyrophosphate, 2 mM EDTA, 1x Sigma protease inhibitor cocktail). Cells were lysed by passing through a 25G1 needle eleven times (BD PrecisionGlide) followed by centrifugation for 20 min at 14,000xg to remove cell debris.

**Western Blotting.** Cell lysates were mixed with 2xSDS sample buffer and boiled for 5 min. Proteins were resolved on SDS-PAGE and transferred onto PVDF membrane (Millipore), followed by incubation with various antibodies. Detection of horseradish peroxidase-conjugated secondary antibodies was performed with Western Lightning<sup>TM</sup> Chemiluminescence Reagent Plus (Perkin Elmer). Results were developed on x-ray films and scanned with an Epson scanner (Perfection 2400).

**Vesicle Preparation.** Lipids in chloroform (0.5 µmol total) were dried under nitrogen gas, and resuspended in 300 µL vesicle buffer (10mM Tris·HCl pH 8.0, 150mM NaCl) to a final concentration of 1.66 mM. Vesicles were formed by water bath sonication followed by probe sonication. Unilamellar vesicles were collected as the supernatant after ultracentrifugation at 194,398xg in a TLA100.3 rotor for 2hr at 25°C. Lipid compositions for the phosphoinositide vesicles were 5% PI(3)P, PIP<sub>2</sub>, or PIP<sub>3</sub>, 95% phosphatidylcholine (PC) as a carrier, 0.05% biotin-phosphatidylethanolamine (biotin-PE) for immobilization of the vesicles on imaging surface, and 0.1% C-18 DiD for

fluorescence imaging of the vesicles. The composition of PA vesicles was similar as above except with 20% PA and 80% PC. Vesicles were diluted 500-fold to yield ~700 vesicles per  $4,500 \mu\text{m}^2$ , loaded into imaging chamber, and incubated for 20 min before loading of cell lysates.

**Single-Molecule Co-localization.** The percentage of colocalization between vesicles and proteins was quantified by determining the number of spots,  $S$ , and position of each DiD and GFP spot present in the same imaging region. Positions of DiD and GFP spots were determined to 2-pixel accuracy by fitting a Gaussian point spread function. Spots lying within 2-pixel distance (pixel size, 133 nm) were considered to be co-localized. The percentage of GFP-positive spots that overlapped with DiD spots was calculated. To determine false co-localization by chance, two different regions were imaged for DiD and GFP, and similar analysis was performed. Co-localization by chance was observed to be ~6%.

**Single-Molecule Analysis for Assembly Plots.** After addition of cell lysates into imaging chambers, several movies (frame rate = 100 msec) were recorded at different incubation times. The first 50 frames were taken with 640-laser excitation to localize DiD-labeled vesicles, followed by 488-laser excitation to detect GFP molecules. Single-molecule fluorescent traces obtained from the movies were divided in three different categories: empty vesicles (only DiD signal), bound vesicles (DiD and GFP signals), and non-specifically bound GFP (only GFP signal). The fraction of bound vesicles was calculated as a percentage of total labeled vesicles. GFP signal from the ‘bound vesicles’ category was further analyzed by Chung-Kennedy filtration algorithm to remove noise. Filtrated traces were manually scored for the number of bleaching steps to determine the number of GFP molecules per vesicle,  $N_{GFP}$ . The fluorescence traces were classified as having 1–10 bleaching steps. Number of GFP molecules per vesicle,  $N_{GFP}$ , at different incubation times was used to build the assembly plots as a distribution of total labeled vesicles. To determine the stoichiometry of vesicle-free proteins, GFP-LBDs in cell lysates were captured using biotinylated GFP antibodies immobilized to the surface via biotin-NeutrAvidin interaction. Copy number of GFP was determined by single-step photobleaching analysis and classified as having one to four bleaching steps or was discarded if no clean bleaching steps could be identified.

## SUPPLEMENTARY FIGURES

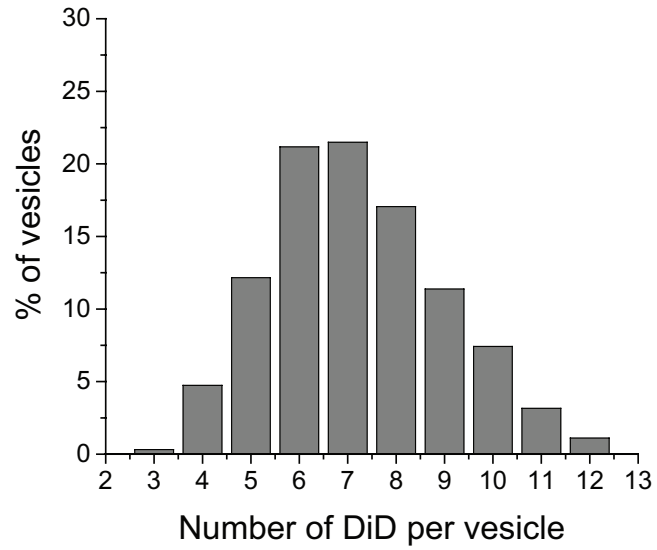


**Figure S1. Number of DiD molecules per vesicle.** Vesicles (containing biotin-PE) were captured on the surface via biotin-NeutrAvidin interaction. The number of DiD molecules was determined by fluorescent photobleaching analysis after laser excitation at 640 nm.

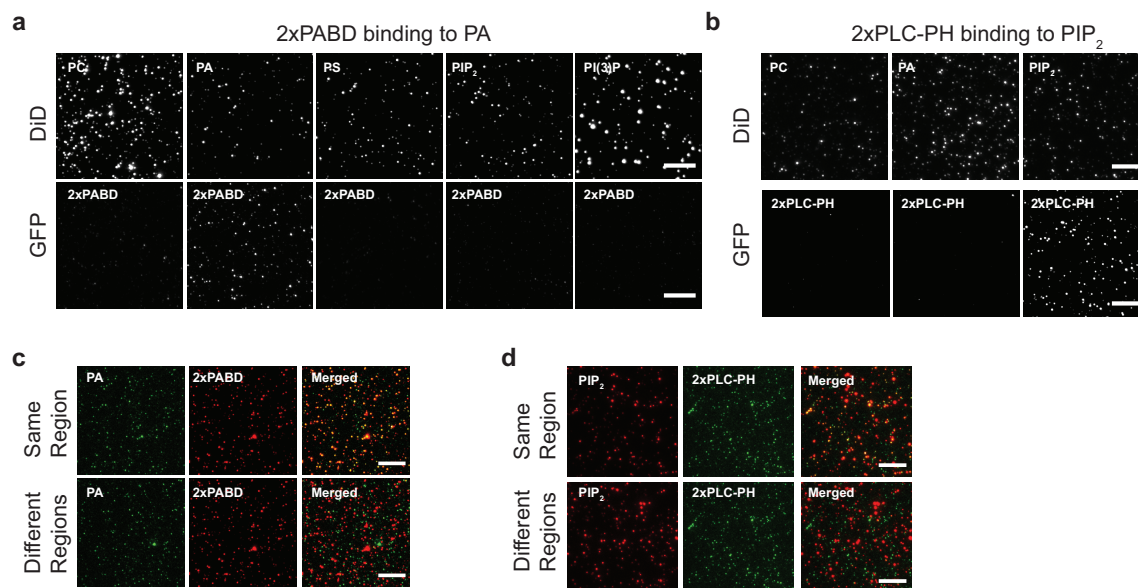


**Figure S2. Binding of tandem-repeat LBDs to their target lipids.** TIRF images for LBD-vesicle pairs are shown. Vesicles were detected via DiD, and LBDs via GFP. (a) 2xPABD and PA. (b) 2xPLC-PH and PIP<sub>2</sub>. (c,d) Overlay of LBDs and vesicles from the same region or different regions. Scale bars: 10 μm.

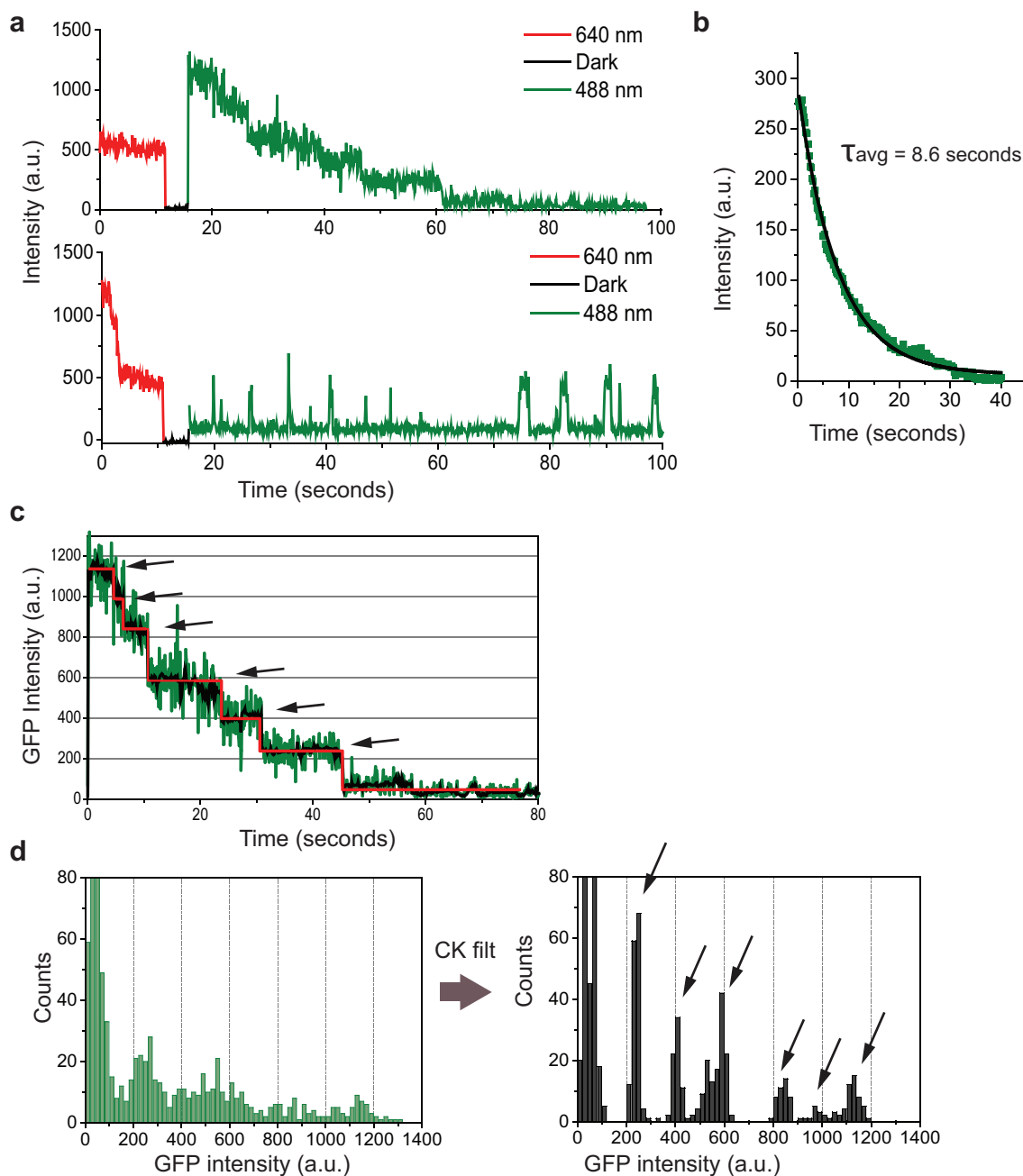


**Figure S3. Framework for data analysis.** (a) Single-molecule fluorescent traces of DiD-labeled vesicles (red lines, 640 nm excitation) and GFP-LBD (green lines, 488 nm excitation) are shown for stable (top panel) and transient (bottom panel) interactions. (b) GFP photobleaching curve. (c) Identification of 6 photobleaching steps (arrows indicate photobleaching steps) after CK filtration (red line). Raw single-molecule traces are shown in green. (d) Histogram of GFP fluorescence intensity before (left) and after (right) CK filtration. Arrows indicate photobleaching steps.

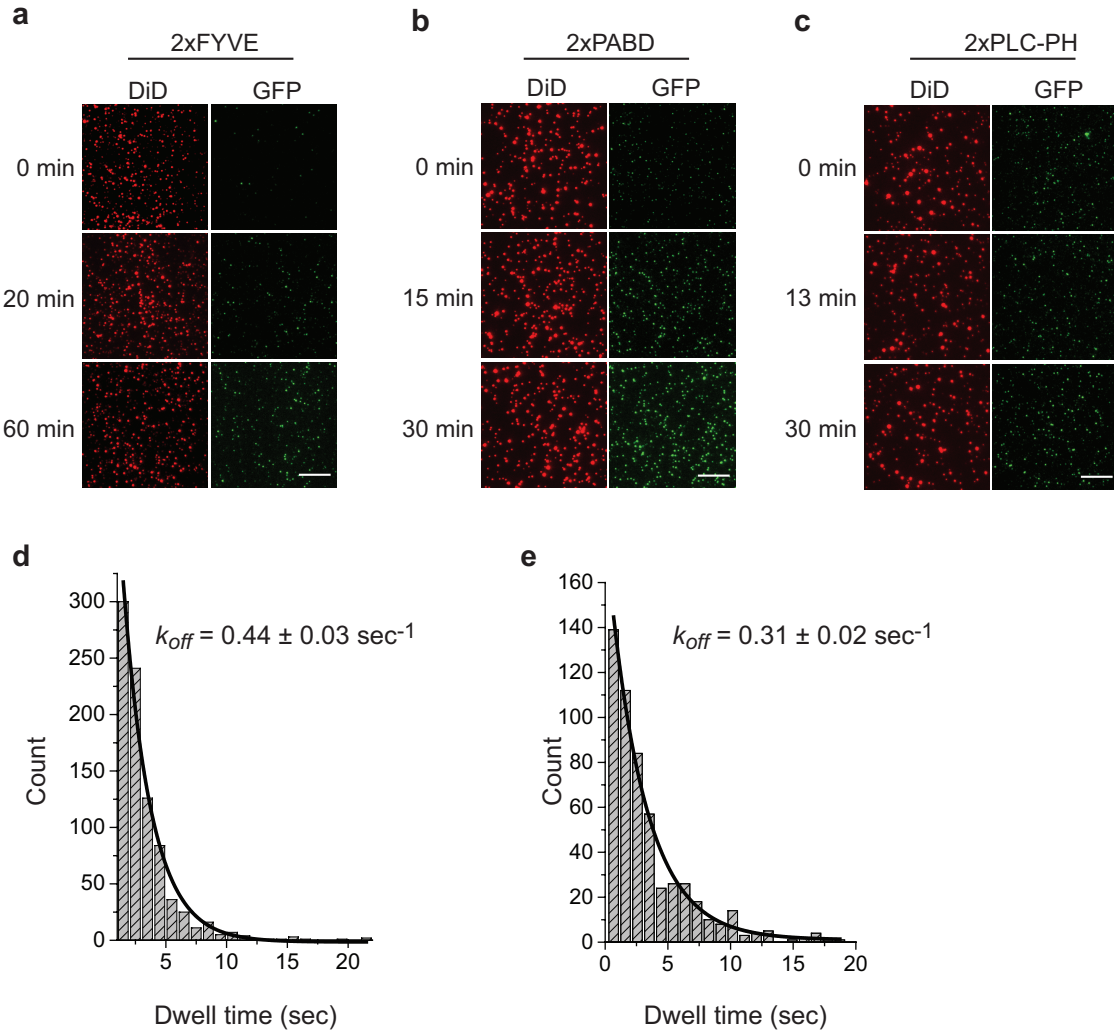


**Figure S4. Binding of tandem LBDs to their target lipids.** (a) TIRF images of DiD vesicles and GFP-2xFYVE bound to PI(3)P vesicles at 3 incubation times. (b) Similar to (a), for binding of 2xPABD to PA vesicles. (c) Similar to (a), for binding of 2xPLC-PH to PIP<sub>2</sub> vesicles. Scale bars: 10 $\mu$ m. (d, e) Dwell time histograms of (d) 2xFYVE transiently bound to PI(3)P and (e) 2xPLC-PH transiently bound to PIP<sub>2</sub> were fitted to exponential decay to yield dissociation rate constants ( $k_{off}$ ).

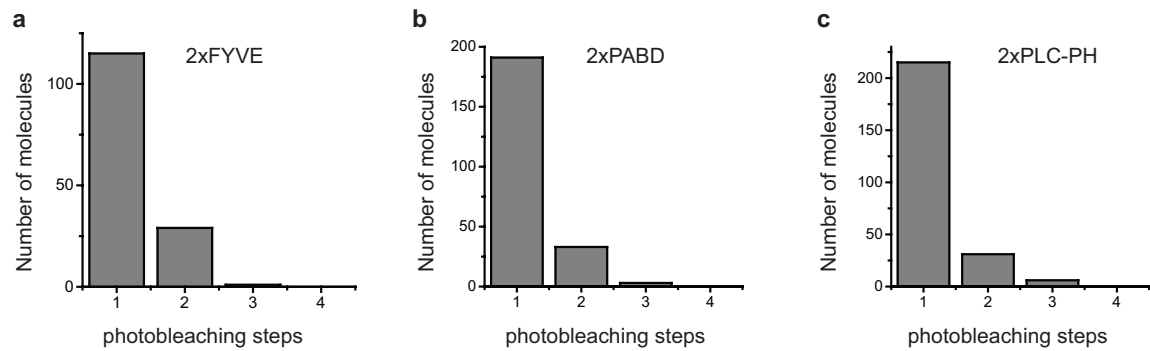


**Figure S5. Tandem-repeat LBDs are mostly monomeric.** GFP-fusion of 2xFYVE (a), 2xPABD (b), and 2xPLC-PH (c) were captured from cell lysates using a biotinylated anti-GFP antibody, followed by GFP photobleaching step analysis.

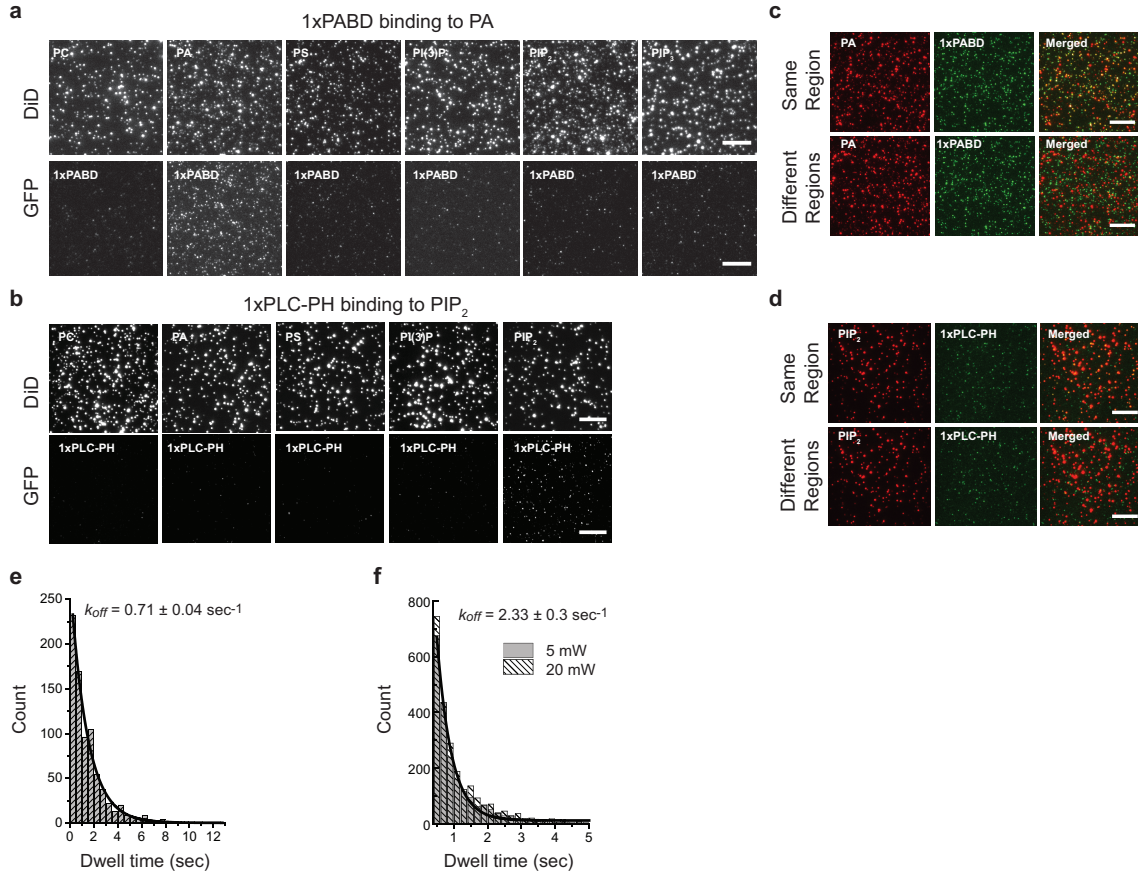


**Figure S6. Binding of single-copy LBDs to their target lipids.** TIRF images for 1xLBD-vesicle pairs are shown. Vesicles were detected via DiD, and 1xLBDs via GFP. (a) 1xPABD and PA. (b) 1xPLC-PH and PIP<sub>2</sub>. (c,d) Overlay of 1xLBDs and vesicles as indicated from the same region or different regions. Scale bars: 10 $\mu$ m. (e) Dwell time histogram of 1xPABD transiently bound to PA was fitted to exponential decay to yield dissociation rate constant ( $k_{off}$ ). (f) Similar to (e) for 1xPLC-PH transiently bound to PIP<sub>2</sub>.

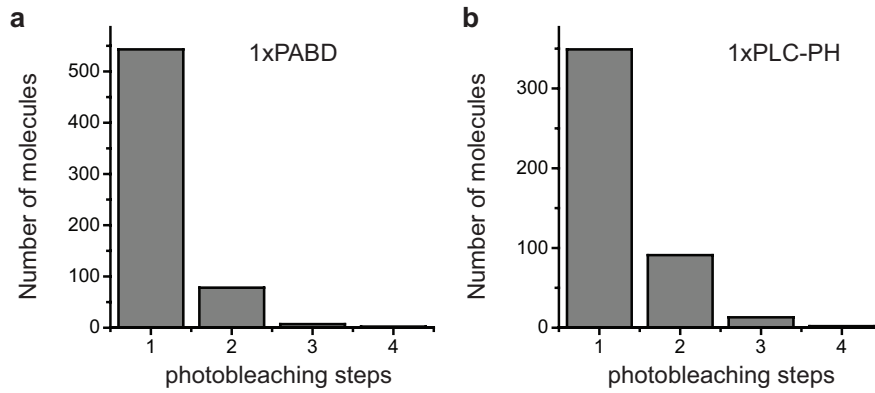


**Figure S7. Single-copy LBDs are mostly monomeric.** GFP-fusion of 1xPABD (a) and 1xPLC-PH (b) were captured from cell lysates using a biotinylated anti-GFP antibody, followed by GFP photobleaching step analysis.

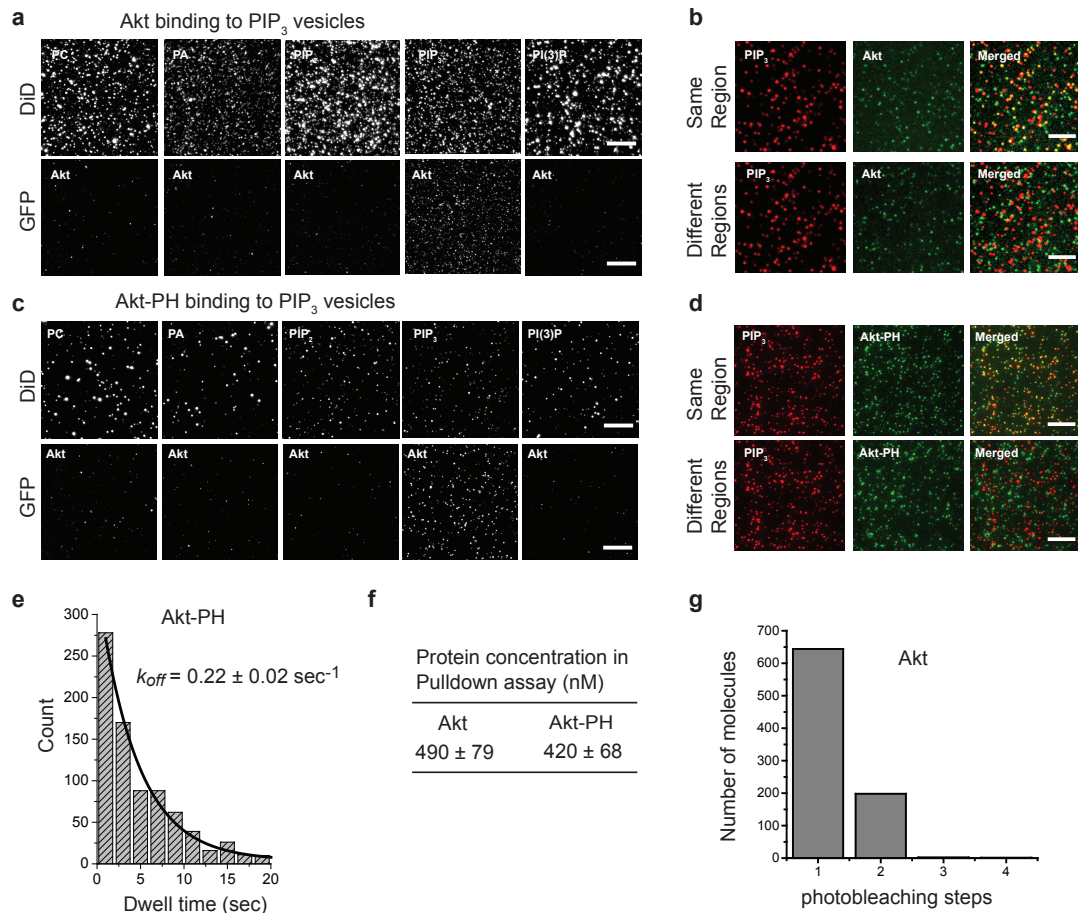


**Figure S8. Binding of Akt and Akt-PH to PIP<sub>3</sub> vesicles.** (a) TIRF images for Akt (GFP) and PIP<sub>3</sub> (DiD) vesicle are shown. (b) Overlay of Akt and PIP<sub>3</sub> images from the same region or different regions. (c) TIRF images for Akt-PH (GFP) and PIP<sub>3</sub> (DiD) vesicle are shown. (d) Overlay of Akt-PH and PIP<sub>3</sub> images from the same region or different regions. (e) Dwell time histogram of Akt-PH transiently bound to PIP<sub>3</sub> vesicles were fitted to exponential decay to yield the dissociation rate constant ( $k_{off}$ ). (f) The concentrations of Akt and Akt-PH in the pulldown assays were determined by single-molecule pulldown of GFP, with purified recombinant GFP as a reference. (g) GFP-Akt captured by anti-GFP antibody was analyzed for photobleaching steps. Scale bars: 10 $\mu$ m.

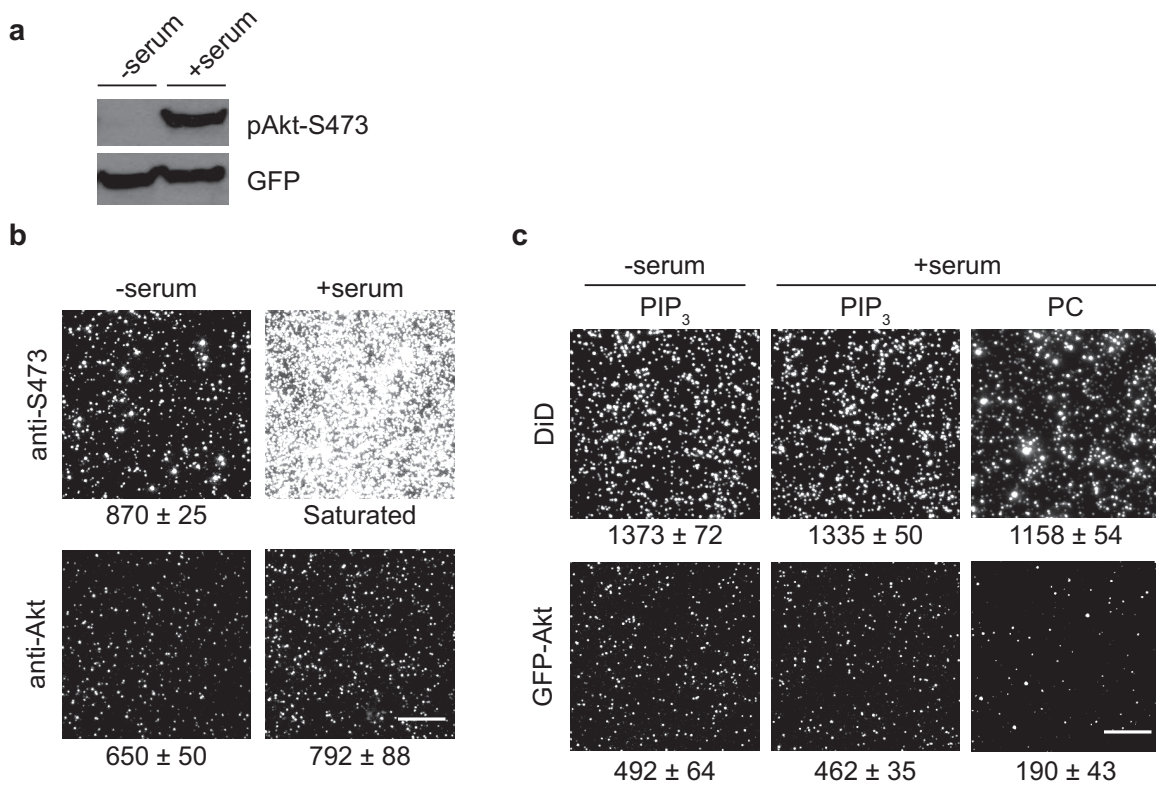


**Figure S9. Serum stimulation does not affect Akt-PIP<sub>3</sub> interaction.** Cells were serum-starved overnight and then stimulated with 10% FBS for 30 min prior to lysis. (a) Expression and S473 phosphorylation of GFP-Akt were determined by western blotting. (b) Akt was captured from cell lysates by either an anti-pS473 antibody or an anti-GFP antibody. (c) Akt was captured from cell lysates by PIP<sub>3</sub> vesicles, with PC vesicles as negative control. The average number of fluorescence spots per imaging area ± SD (n=10 images) is shown under each image.

## SUPPLEMENTARY REFERENCES

- (1) Gillooly, D. J.; Morrow, I. C.; Lindsay, M.; Gould, R.; Bryant, N. J.; Gaullier, J. M.; Parton, R. G.; Stenmark, H. *EMBO J* **2000**, *19*, 4577-4588.
- (2) Zeniou-Meyer, M.; Zabari, N.; Ashery, U.; Chasserot-Golaz, S.; Haeberle, A. M.; Demais, V.; Bailly, Y.; Gottfried, I.; Nakanishi, H.; Neiman, A. M.; Du, G.; Frohman, M. A.; Bader, M. F.; Vitale, N. *The Journal of biological chemistry* **2007**, *282*, 21746-21757.
- (3) Botelho, R. J.; Teruel, M.; Dierckman, R.; Anderson, R.; Wells, A.; York, J. D.; Meyer, T.; Grinstein, S. *J Cell Biol* **2000**, *151*, 1353-1368.
- (4) Bohdanowicz, M.; Cosio, G.; Backer, J. M.; Grinstein, S. *J Cell Biol* **2010**, *191*, 999-1012.
- (5) Watton, S. J.; Downward, J. *Curr Biol* **1999**, *9*, 433-436.